International Journal of Adhesion and Adhesives xxx (xxxx) 102849

Contents lists available at ScienceDirect

International Journal of Adhesion and Adhesives

journal homepage: www.elsevier.com/locate/ijadhadh

Analysis of contact area in a continuous application-and-peel test method for prepreg tack

G.Y.H. Choong, A. Endruweit, D.S.A. De Focatiis *

Faculty of Engineering, University of Nottingham, Nottingham, NG7 2RD, United Kingdom

ARTICLE INFO

Keywords:
Tack
Epoxides
Peel
Prepreg

ABSTRACT

The relationship between prepreg tack and the degree of intimate contact (DoIC) between prepreg and a rigid substrate was explored in the context of a continuous application-and-peel test method. Tack for a unidirectional prepreg tape was characterised for different surface combinations and varying test parameters (material feed rate, temperature) at a constant compaction pressure. Application of the prepreg to a transparent rigid substrate (glass), was carried out at matching test conditions to the prepreg tack measurements. Optical microscopy was utilised to acquire images of the contact area at the prepreg-glass interface. Image analysis of the micrographs enabled quantification of the contact area. The time- and temperature-dependent viscoelastic behaviour of the resin was explored directly on the prepreg using oscillatory parallel plate rheometry, and time-temperature superposition was applied to construct both tack and DoIC master curves. The shifted DoIC data showed that true contact area increases with decreasing shifted feed rates, until maximum contact area is achieved. Similarly, tack increases with decreasing shifted feed rates. However, at a critical feed rate, the bond failure mechanism switches from adhesive to cohesive failure. In cohesive failure, tack decreases with decreasing feed rate despite the high levels of DoIC.

1. Introduction

In Automated Material Placement (AMP), robotic machinery is used to place layers of unidirectional fibre tape pre-impregnated with a partially cured thermoset resin, known as a prepreg and commonly made from carbon fibre and epoxy resin, on a tool surface to lay up laminates. This type of process is typically used for the manufacture of large composite components with low geometrical complexity, in particular for aerospace applications, e.g. wings or fuselage sections.

AMP process variants are Automated Tape Laying (ATL), where prepreg tapes have widths in the order of several inches, or Automated Fibre Placement (AFP), where widths are smaller than one inch. In AFP, material deposition rates are typically lower than in ATL, but narrow tapes are more suitable for deposition along curved paths. For both variants, process parameters such as deposition rate, temperature and applied pressure can be adjusted. Effective use of AMP is reliant on the understanding of prepreg material characteristics in order to identify optimal deposition parameters with respect to speed, quality of bond and absence of defects. Once a laminate is laid up with the required number of layers and orientations, it is processed in an autoclave at high temperature (to induce resin cure) and pressure (for consolidation). Thus, prepreg materials are required to have sufficient adhesive properties to maintain a prescribed geometry prior to autoclave processing.

The lay-up performance, for a given set of process parameters, is strongly related to the level of adhesion, or tack, between (1) the prepreg and the tool surface, (2) successive prepreg plies and (3) the prepreg and the placement head roller. While high tack between prepreg tape and roller may result in prepreg sticking to and wrapping around the roller, insufficient tack between plies and/or between prepreg and tool contributes to the formation of defects in the lay-up, such as wrinkling and bridging [1]. It is essential to maintain sufficient adhesion prior to curing to reduce the likelihood of defect formation that may affect the final properties of the cured component. Characterisation of prepreg tack is therefore critical for the optimisation of AMP processes [1].

An approach to understanding tack phenomena is investigation of the evolution of the contact area between the prepreg and its mating surface. One of the earliest studies of prepreg tack by Gillanders et al. [2] explored the correlation between tack strength (defined as the tack

* Corresponding author.
E-mail addresses: gabriel.choong@nottingham.ac.uk (G.Y.H. Choong), andreas.endruweit@nottingham.ac.ukand (A. Endruweit), davide.defocatiis@nottingham.ac.uk (D.S.A. De Focatiis).

https://doi.org/10.1016/j.ijadhadh.2021.102849
0143-7496/© 2021

force per unit probe area) and contact area using an inverted probe technique in which the probe compression and retraction phases were controlled. Images of the contact area between prepreg and a glass substrate were acquired after compression. The true contact area of the bond created under varying conditions of contact time and pressure was determined from the images. For the prepreg examined, a strong correlation between tack strength and contact area was observed.

The relationship between tack strength and contact area has been widely investigated to shed light onto bonding and debonding mechanisms in pressure sensitive adhesives (PSAs) [3–5]. Common experimental methods for investigating PSAs are the probe tack test and the peel test. In the case of probe tests, real-time direct observation of the deformation process of a PSA film was realised using the inverted probe technique proposed by Lakrout et al. [3]. This makes use of a mirror positioned at 45° to the contact plane allowing visual observation of the contact of the PSA film bonded to a glass slide. This experimental setup was able to record (1) the true contact area between the probe and the film and (2) the cavitation and fibrillation processes during the debonding of the film from the glass surface. The contact area patterns associated with the debonding processes could then be related to specific points on the adhesive's stress-strain curve. Horgnies et al. [4] employed a peel test to observe the fibrillation of a PSA bonded to a glass substrate under controlled force and time. Here, the contact area formed was captured on optical micrographs, and fibrillation was observed from the side during the peeling stage, enabling the authors to confirm that debonding energy increases with increasing contact area.

In both of these prior studies, the bond is formed as a separate process to the debonding stage. Recently, a continuous application-and-peel method of measuring tack force was developed by Crossley et al. [6] as a means of obtaining a measure of bond quality of relevance to AMP processes. In this method, a prepreg tape is pressed onto a substrate and peeled in the same process at a constant rate and temperature. Using this method and a process of time-temperature superposition (TTS) based on resin viscoelasticity, Crossley and co-workers [7] were able to produce tack mastercurves in which a maximum tack force can be observed at the transition between adhesive and cohesive failure of the bond. The method was later used by Endruweit et al. [8] on unidirectional carbon fibre/epoxy prepregs to study the effect of different surface combinations, material out-time, humidity and compaction force, and by Smith et al. [9] for a study of woven carbon fibre/epoxy prepreg tack subjected to varying material out-times.

In an effort to study inter-ply void formation in out-of-autoclave prepregs, Helmus et al. [10] proposed an experimental setup comprising of a vacuum bagging arrangement using a glass tool, with a camera located underneath the tool to acquire macroscopic images of the contact area between the prepreg and the transparent tool. The images were post-processed and binarised to analyse the contact patterns as a function of time, up to the end of the curing cycle. This technique provided a quantitative measurement of the evolution of the contact area during the manufacturing process over a large sample area.

The aim of this work is to employ the established contact area imaging and processing techniques in the context of the continuous application-and-peel tack measurement method for prepregs. The goal is to investigate the role of contact area on tack in a test method relevant to AMP processes. The continuous application-and-peel tack testing fixture [7] is employed to create a contact between prepreg and a rigid glass substrate at a range of temperatures and rates, but without the subsequent peel stage. The interfaces between glass substrates and prepregs are then imaged using optical microscopy, and image processing is applied to obtain measurements of the true contact area. Complementary measurements, which include the continuous peel stage, are carried out under identical conditions to determine prepreg tack on both rigid substrates and on prepreg substrates. Both the tack and the contact area data are reduced to master curves using TTS, with parameters determined from the resin viscoelastic behaviour.

2. Materials

A Hexcel 180°C cure epoxy developmental system was used for all tack testing and contact area investigations in this work. The material system consists of unidirectional carbon fibre reinforcement and epoxy resin. The material has two distinguishable faces. One face is covered with a protective backing paper which is removed just prior to tack measurements. The face on the opposite side has no protective paper. In the following, the faces will be referred to as P ("paper") or N ("no paper").

3. Experimental methods

3.1. Tack measurement: continuous application-and-peel method

Prepreg tack was measured employing the continuous application-and-peel method and test fixture described in Crossley et al. [6]. The tack test fixture is mounted on the base of a universal testing machine, equipped with an environmental chamber. Fig. 1 shows a schematic diagram representing the continuous motion prepreg tack test and a typical specimen assembly arrangement for determining tack between the prepreg and the rigid substrate. The prepreg N and P faces are in contact with the substrate and the protective film, respectively. The protective film prevents the transfer of resin from the prepreg to the peel roller. The specimen assembly is then loaded into the tack test fixture where the combination of stiff peel and compaction rollers presses the prepreg against the substrate at a fixed pre-determined force. The free end of the prepreg specimen is attached to the cross-head and load cell of the testing machine using a material clamp, such that the prepreg is forced to bend 90° around the peel roller. In a tack test, the cross-head movement translates into a horizontal movement of the specimen assembly, pulling the assembly through the fixture rollers. As a result, the prepreg is first bonded to, and subsequently immediately peeled from the substrate in a single continuous process at a feed/peel rate that corresponds to the cross-head speed. Here, the duration of compaction is

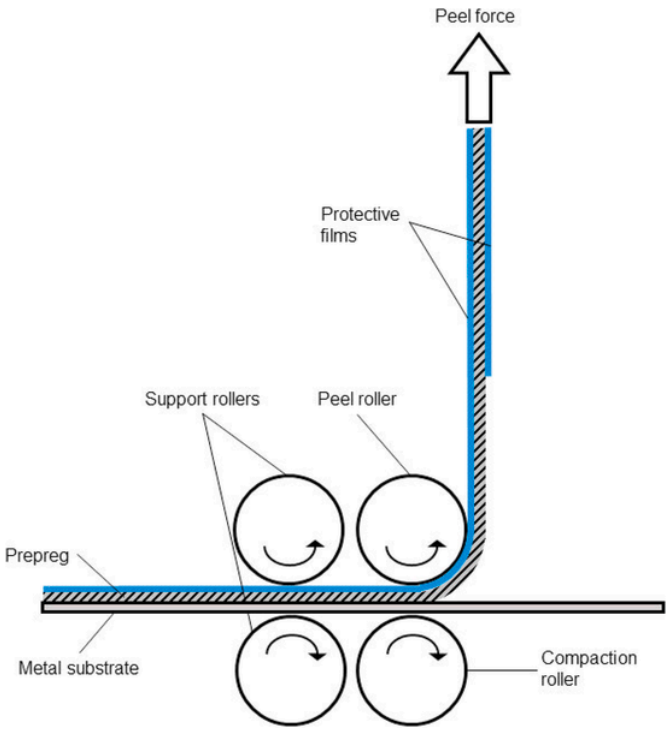

Fig. 1. Schematic of the continuous application-and-peel test method to determine tack between the prepreg and the steel substrate, illustrated undergoing the second (peel) phase.

not controlled directly, but is effectively inversely proportional to the feed rate.

The tack measurement itself is divided into two phases. In the first phase, a second protective film covers the underside of the prepreg and prevents adhesion to the substrate. Hence, only the force required to overcome the dissipative effects arising from friction and from bending the prepreg ply around the peel roller, F_{diss}, is recorded. In the second phase of the test, where the exposed part of the prepreg surface is in contact with the substrate, the measured force, F_{peel}, corresponds to the sum of $F_{diss,}$ the force for bending a single layer of protective film, and the tack force, F_t. In a separate test, a single layer of protective film is laid up on a metal substrate, and the average force for bending of the film around the peel roller, F_b is measured. Hence, the average tack force F_t can be found from the difference between F_{peel} and $F_{diss,}$ and the addition of F_b. Examples of raw force-displacement curves for tack tests of various prepreg materials can be found in Refs. [6,8,9] and in Appendix A.

In this study, tack measurements were performed for two surface combinations: prepreg-steel (representative of the contact with tooling) and prepreg-prepreg (representative of the interfaces within a layup). For the first surface combination, a rectangular prepreg specimen is cut to a length of 215 mm and a width of 75 mm and laid up by hand on a rectangular steel substrate (140 mm × 80 mm) such that one end of the specimen is flush with the edge of the substrate. For the second surface combination, an additional prepreg specimen (140 mm × 75 mm) is bonded to the steel substrate using double-sided adhesive tape (3 M High performance Double Coated Tape 9088). The role of the double-sided adhesive is to ensure that the bond between the metal substrate and the prepreg is stronger than the bond between the two prepreg layers, enabling the weaker bond to be studied. For both surface combinations, an additional protective film (135 mm × 75 mm) is positioned on the face of the rectangular prepreg such that an 80 mm length of the exposed surface is in contact with the prepreg layer that is bonded to the metal substrate, in order to enable F_{diss} to be recorded in the absence of tack.

The compaction force is defined as the normal force applied through the compaction roller and peel roller. The springs connecting the rollers are set such that a compaction force of 100 N is applied across the width of the contact when the assembly passes through the rollers. At this level of compaction force, tack has been shown to be independent of compaction force [8]. Separate series of tests were carried out at test temperatures, T, of 10 °C, 20 °C, 30 °C, 40 °C and 50 °C. The surface temperature of the laid-up specimen was monitored using a non-contact infrared thermometer, and tests were started when the temperature was within ±1 °C of the target temperature. Cooling the environmental chamber below ambient temperature was performed using liquid nitrogen. The crosshead speeds, and hence feed rates, r, employed for each test temperature were 50 mm min^{-1}, 150 mm min^{-1}, 300 mm min^{-1}, and 500 mm min^{-1}. The humidity in the environmental chamber for all tests was recorded, as this is known to have some effect on tack [8], but could not be controlled.

3.2. Application of prepreg to substrate surfaces

In order to evaluate the degree of intimate contact, DoIC, between the prepreg and substrate surfaces for tack measurements, the prepregs were pressed against glass surfaces at conditions matching the tack tests. Modifications to the methodology described in Section 3.1 included the specimen preparation and assembly stage, and the exclusion of the peel phase of the tack test. For the specimen assembly preparation, as illustrated in Fig. 2(a), each metal substrate was fitted with three plain glass microscope slides (ground, 90°) arranged in parallel, across the width of the substrate. Glass slides were used as substrates to facilitate image acquisition of the interface between prepreg and substrate surface. Dimensions of the glass slides were 76 mm × 26 mm, with a thickness ranging between 1.0 mm and 1.2 mm. For each test condition, a prepreg specimen of dimensions 60 mm × 25 mm was positioned on top of each of the three glass slides, with the prepreg N faces in contact with the glass surfaces. A long protective film (215 mm × 75 mm) was secured at the back edge of the metal substrate. The specimen assembly consisting of the prepregs, glass slides and protective films was inserted into the tack fixture with the front edge of the protective film secured to the material clamp, enabling the assembly to be compressed by the compaction roller under controlled temperature and rate. Fig. 2(b) presents a schematic diagram of the specimen assembly during compaction as the assembly passes through the fixture rollers.

The microscope slides in contact with the prepregs were carefully removed from the metal substrate after compaction. Specimen assemblies prepared at elevated temperatures were set aside to cool to ambient temperature for a few minutes after removal from the environmental chamber, to protect the established contact pattern. The glass slides were then transferred to an optical microscope to examine and record the contact area, typically within 5 min of compaction. A further 10 min was required to acquire all the contact area images for each test condition.

3.3. Optical microscopy and image analysis procedure

The contact area developed between the prepreg and glass surface was investigated using bright-field microscopy in reflection mode. An Olympus BX51 microscope equipped with an Infinity 2 digital camera was used to capture the contact area at low magnifications (4x). An acrylic template with a cavity to locate a glass slide was fixed to the microscope stage and employed to position each glass slide for image acquisition at six repeatable positions. Each micrograph provided an image of area of ~15 mm^2, at a resolution of 2448 × 2048 pixels. Images were acquired through the glass slides, which allowed the contact area to be identified based on the grayscale levels. Owing to the similar refractive indices of glass and epoxy resin, areas of intimate contact appear darker as the interface is transparent, while reflections occur at the interface where intimate contact has not been established, as was also observed by Helmus et al. [10].

All images were processed using Matlab to determine the DoIC between the prepreg and glass surface. Fig. 3 illustrates these image processing steps for a representative micrograph. The first step involved converting the micrograph to a greyscale (8-bit) image. In order to remove non-uniform background illumination at the edges of the micrographs, an identical region of interest (ROI) was identified for all micrographs to avoid arbitrary cropping of the images. A circular shape corresponding to an area of ~9.5 mm^2 was selected as the ROI with uniform illumination, with the centre of the circle coinciding with the centre of the micrograph. The histogram of the ROI is then computed and utilised to determine the threshold value to create a binary image that is employed to determine the DoIC. Each test condition was represented by 18 images obtained from 6 locations on 3 slides, which provided a total area of 171 mm^2 for analysis.

The histograms for the greyscale image were modified to exclude the frequency count from the two extreme grey values, which are black and white pixels corresponding to grey values 0 and 255, respectively, when identifying the threshold value. The features of interest in the micrographs do not relate to these grey values. For each micrograph, there are commonly three dominant intensities (shades of grey) that correspond to: (1) the contact of the resin with the glass (darkest shade); (2) the fibres coated in resin that are not in contact with the glass (intermediate shade); and (3) regions of high concentration of resin that are not in contact with the glass (lightest shade). Comparable dominant intensities were observed in micrographs of prepreg surfaces for dissimilar UD tapes [8]. Depending on the compaction conditions in this work, the contact area patterns between the prepreg and glass slide produced

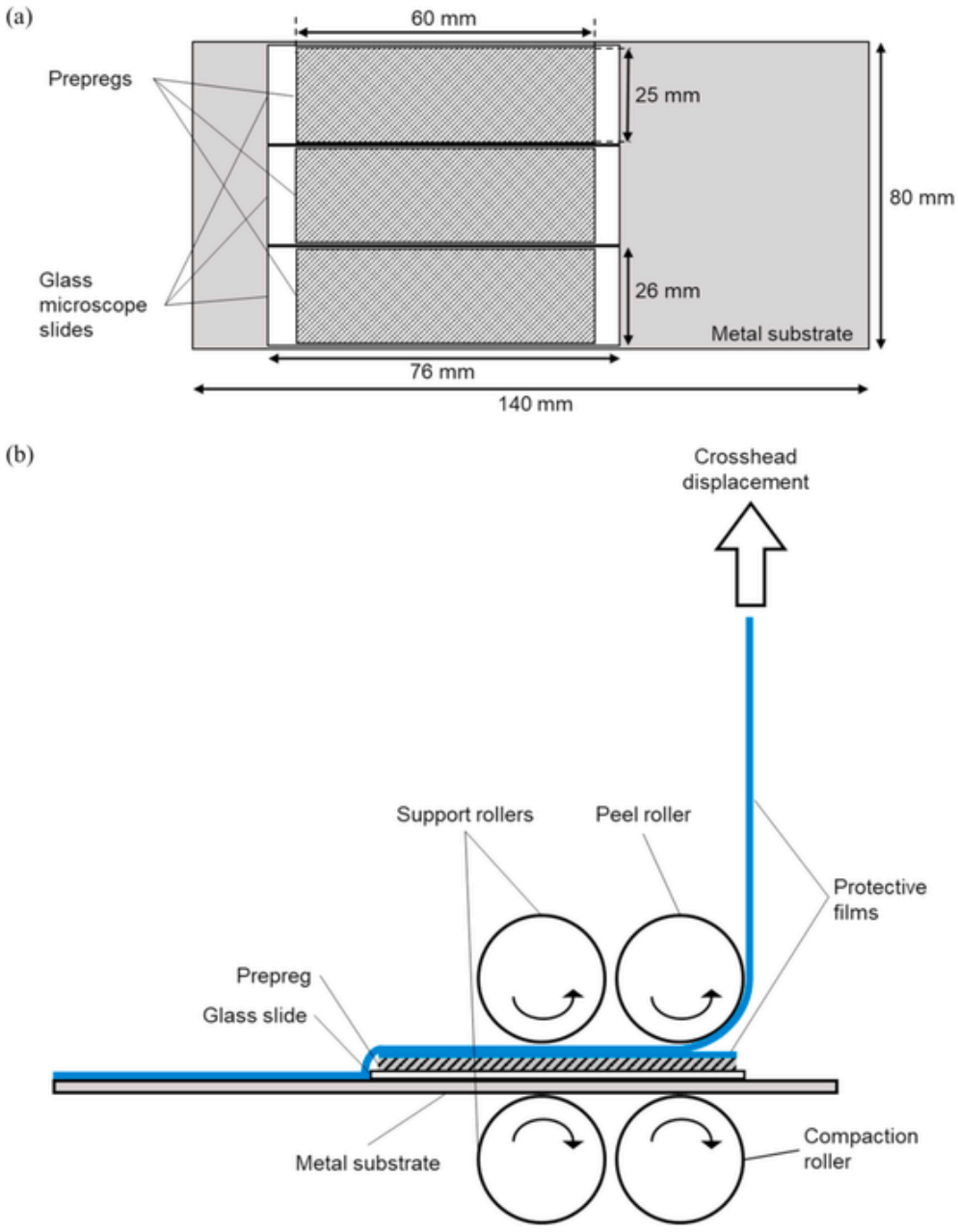

Fig. 2. (a) Specimen assembly for compacting the prepreg against the glass surface (the left edge is the leading edge of the assembly). (b) Schematic of the use of the tack testing fixture without the peel phase, enabling compaction only of the specimen assembly.

different histogram shapes. For bimodal and trimodal histograms, the threshold value was determined as local minimum associated with the histogram valley between the peaks for dominant intensities relating to (1) and (2). For unimodal histograms with a single dominant greyscale value, the centre of the greyscale at 128 was used as the threshold value, as no local minimum could be identified. The latter histogram shape concerns conditions of both near-complete contact and very low contact; this choice of threshold does not have a significant effect on the value of DoIC determined. In order to determine the DoIC for each binarised image (composed only of black or white pixels), the count of black pixels in the circular ROI was divided by the total pixel count in the same ROI.

3.4. Rheometry

Isothermal frequency sweeps were performed using an Anton Paar MCR 302 rheometer fitted with a CTD 450 environmental chamber and a Grant Instruments LTD6 refrigerated circulator for controlled heating and cooling. Since neat epoxy resin used in the prepreg was not available, frequency sweeps were performed directly on prepreg specimens cut to a size of 30 mm × 30 mm, similar to the procedure carried out in Smith et al. [9]. Although the magnitude of the viscoelastic measurements is strongly affected by the presence and distribution of the fibres in the material, the observed changes in the storage modulus G' with temperature can be attributed primarily to the resin system, since the fibres do not show any significant temperature-dependent behaviour in this temperature range.

All tests were carried out using a standard 25 mm diameter parallel plate geometry in an air atmosphere. At the beginning of each test, the specimen was subjected to a normal force of 20 N at the lowest test temperature. This step promotes contact between the rheometer plates and the specimen prior to setting a fix gap distance. Isothermal frequency sweeps were carried out between 15 °C and 60 °C, in increments of 10 °C from 20 °C onwards, at logarithmically increasing frequencies,

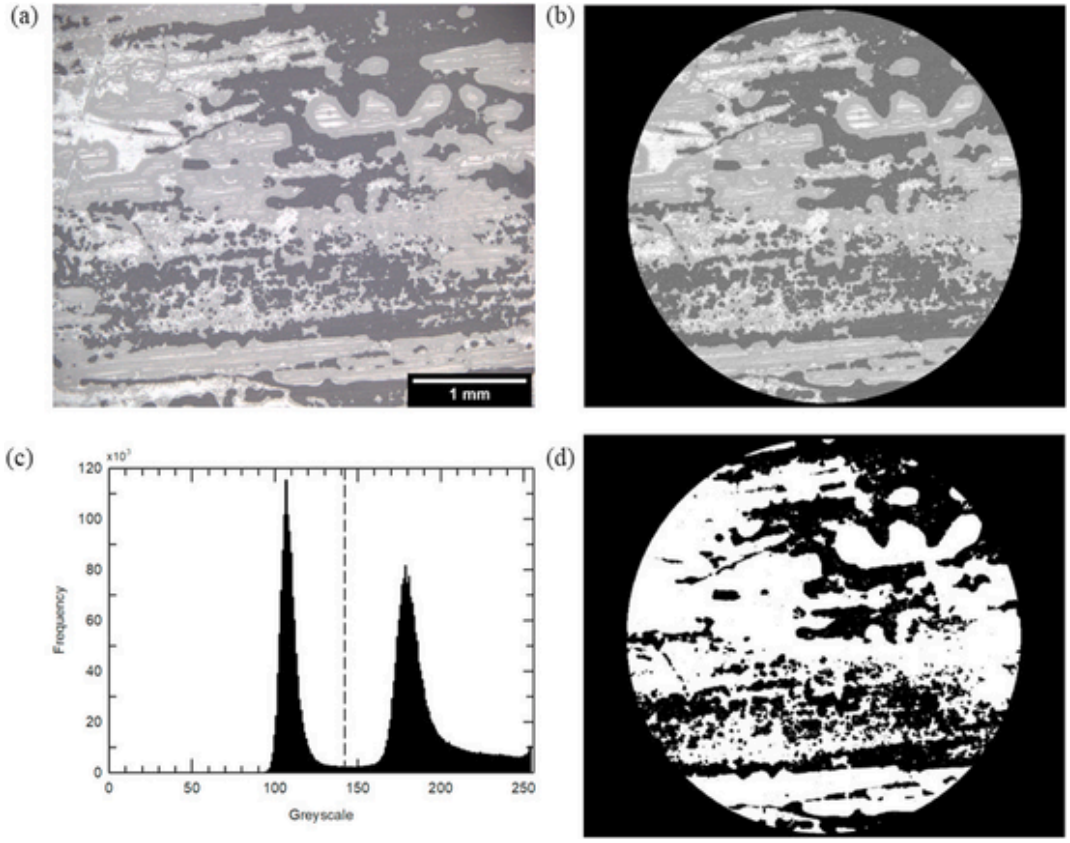

Fig. 3. The image processing approach for a representative micrograph to determine contact area between the prepreg and glass surface. (a) Contact area image corresponding to an application temperature of 10 °C and feed rate of 50 mm/min. (b) Cropped greyscale image showing the region of interest (ROI) used in the analysis. (c) Histogram of image (b) with frequency of pixels for greyscale value 0 (black) and 255 (white) omitted, and showing the local minimum determined as the threshold value of 142 (*dashed line*). (d) Binarised image of (b) using the threshold value identified from (c) corresponding to a DoIC of 39%.

f, from 1 Hz to 100 Hz. The strain amplitude was fixed at a small value of 0.1% to avoid disrupting the fibres.

4. Results

4.1. Time-temperature dependence of the resin properties

Isothermal frequency sweep data was shifted to construct the viscoelastic master curve using an automated procedure that minimises the area enclosed by adjacent frequency sweeps [11], and Fig. 4 reports the shift factors, a_T. The dependence of a_T on temperature at a reference temperature, T_{ref}, can be described by the Williams, Landel and Ferry (WLF) equation [12] given as

$$\log\ a_T = \frac{-C_1\left(T - T_{ref}\right)}{C_2 + \left(T - T_{ref}\right)}. \quad (1)$$

where C_1 and C_2 are empirical constants. Using $T_{ref} = 20$ °C, C_1 and C_2 were determined as 7.07 and 48.56 °C, respectively. The shifting along the frequency axis produces a master curve as illustrated in the inset of Fig. 4, and generally exhibits satisfactory overlap, particularly in G'. Upon closer inspection of the master curve, small deviations from the superposition of the loss modulus, G'' (representing the energy dissipated), are visible in the plateau region at high frequencies. However, considering the complexity of the presence of fibres, and the changes in relaxation modes across the frequency range, the superposition is considered acceptable to provide an insight into time-temperature dependence of the resin. Although rheometry on the prepreg itself is feasible, direct measurement of resin rheology is always preferred.

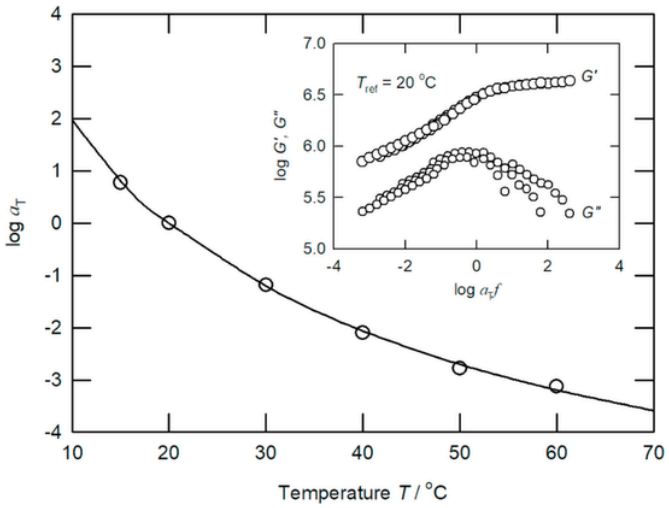

Fig. 4. Horizontal shift factors, a_T, obtained from the prepreg. The *solid line* indicates the Williams-Landel-Ferry equation (Eq. (1)). *Inset* shows the reduced frequency master curve of prepreg at $T_{ref} = 20$ °C.

4.2. Tack master curves

Tack was measured between prepreg and substrate surfaces relevant to AMP. For the prepreg-steel surface combination, tack was measured between the prepreg and a cleaned steel substrate (with ASTM A480 No. 2B surface finish) which represented a flat tooling surface. No release agent or tackifier was applied to the steel substrate. For the

prepreg-prepreg combination, tack between the prepreg layers was measured for surface pairings N on P with aligned plies. The N face of the top prepreg layer of the specimen assembly was in contact with the P face of the prepreg that was bonded to the steel substrate using double-sided adhesive tape, such that the N face of the bottom layer was in contact with the steel substrate. This follows conventional laminate layup where the N face of a prepreg layer is typically in contact with the P face of a previously deposited layer. In such a case, the bond between the prepreg and the steel substrate provided by the double-sided adhesive tape needs to be stronger than the measured tack between the prepreg layers. There was no indication of insufficient bond strength between the bottom prepreg ply and the steel substrate.

As shown for various prepreg systems, the TTS principle is applicable to tack data acquired from continuous application-and-peel tests [7–9], such that the tack force, F_t, measured at temperature, T, and feed rate, r, is equivalent to the tack force at T_{ref} and a shifted feed rate, $a_T r$:

$$F_t(T, r) = F_t\left(T_{ref}, a_T r\right). \tag{2}$$

Employing the WLF shift factors presented in Fig. 4, the feed rates were shifted to T_{ref} = 20 °C to produce the tack master curves for prepreg-steel and for prepreg-prepreg which are plotted in Fig. 5(a) and (b), respectively. The TTS principle enables data acquired at different temperatures to be interpreted in terms of a broader rate range of feed rates than can be explored using a screw-driven testing machine. This means that the procedure is able to provide insight into the applicability of the tack test to deposition rates relevant to AMP processes (of the order of 1 ms^{-1}). Examples of tack process maps can be seen illustrated in Smith et al. [9].

Both tack master curves in Fig. 5 are well described by a Gaussian curve, as previously suggested [8], which is described by

$$F_t\left(T_{ref}, a_T r\right) = F_{t,max}\ \exp\left(-\left(\frac{\log\left(a_T r\right) - \log\left(r_{max}\right)}{w}\right)^2\right). \tag{3}$$

where $F_{t,max}$ is the maximum tack force, r_{max} is the rate at maximum tack at T_{ref}, and w indicates the width of the curve. The coefficient of determination, R^2, is a measure for the quality of the purely phenomenological fit. Both $F_{t,max}$ and r_{max} are determined as quantitative descriptors of tack. Table 1 lists the results characterising the tack behaviour derived from fitting the Gaussian curves to the data. Both $F_{t,max}$ and r_{max} determined for the prepreg-prepreg pairing were higher than for prepreg-steel by factors of 8.4 and 3.8, respectively.

4.3. Contact area between prepreg and substrate surface after compaction

Fig. 6 shows selected optical micrographs representing the evolution of the contact area between the prepreg and glass surface after compaction using the tack fixture at various temperatures and feed rates. Fig. 6(a) is a condition of very low contact area, whereas Fig. 6(b) to 6 (d) illustrate contact patterns with progressively increasing DoIC as temperature increases through to almost complete contact (DoIC ~100%) at the highest test temperature. Closer examination of Fig. 6 (a) and (b) reveals the non-uniformity of local resin distribution indicated by the white areas under reflected light.

Binarising the micrographs using the technique described in Section 3.3 enables quantification of the contact area. Fig. 7(a) presents the average DoIC obtained from five test temperatures each with four feed rates, with error bars representing the standard deviation acquired from 18 separate image locations for each test condition. The shift factors obtained in Fig. 4 are employed to shift the DoIC data along the feed rate axis to T_{ref} = 20 °C. This allows the construction of the DoIC master curve presented in Fig. 7(b). The overall trend reveals increasing DoIC as shifted feed rates decreased (i.e. as temperature increases), with saturation of DoIC at low shifted feed rates.

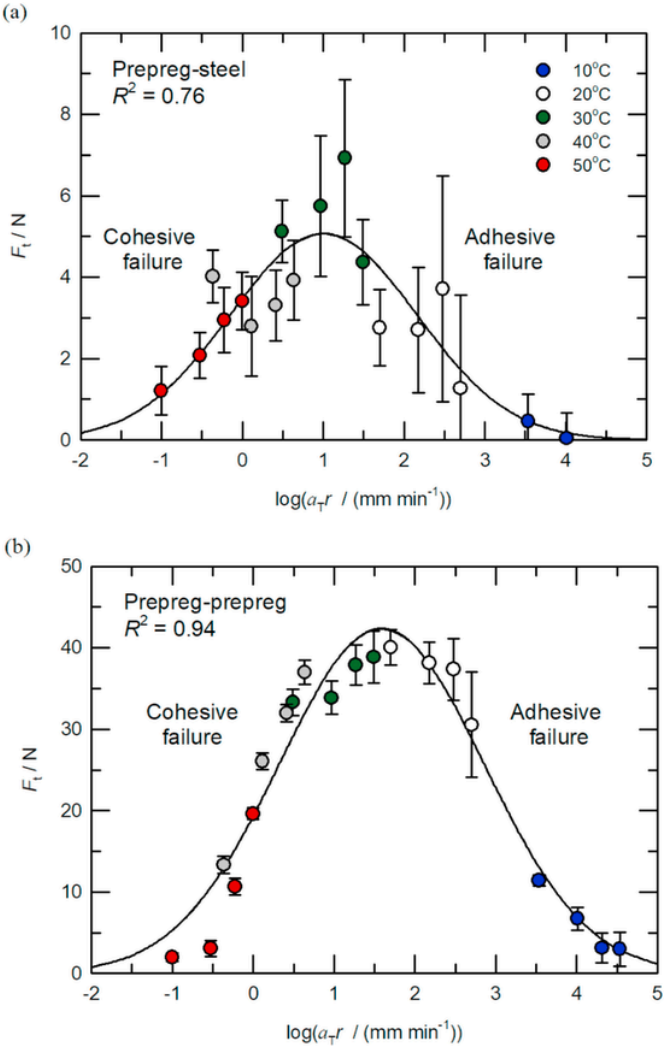

Fig. 5. Tack mastercurves for different surface pairings, based on data acquired at different temperatures, T, and feed rates, r, shifted to a reference temperature T_{ref} = 20 °C; average values and standard deviations are indicated. The *solid lines* represent fits to Eq. (3) with the corresponding coefficients of determination, R^2 shown.

Table 1
Tack data for different surface pairings, shifted to the reference temperature T_{ref} = 20 °C: parameters and standard errors derived from Gaussian fit curves according to Eq. (3), for maximum tack force, $F_{t,max}$, feed rate at maximum tack at T_{ref}, r_{max}, width of curves, w and coefficients of determination, R^2.

Surface pairing	$F_{t,max}$/N	r_{max}/(mm min^{-1})	w	R^2
Prepreg N – steel	5.07 ± 0.53	10.12 ± 1.40	1.63 ± 0.24	0.76
Prepreg N – prepreg P	42.41 ± 1.66	38.74 ± 1.15	1.79 ± 0.09	0.94

5. Discussion

The tack data shows that $F_{t,max}$ for prepreg-prepreg is significantly higher than for prepreg-steel, whilst the shifted feed rate corresponding to $F_{t,max}$ for both surface pairings is of the same order of magnitude. The disparity in $F_{t,max}$ observed for different surface pairings can be attributed to the different bonding behaviour between the resin and substrate

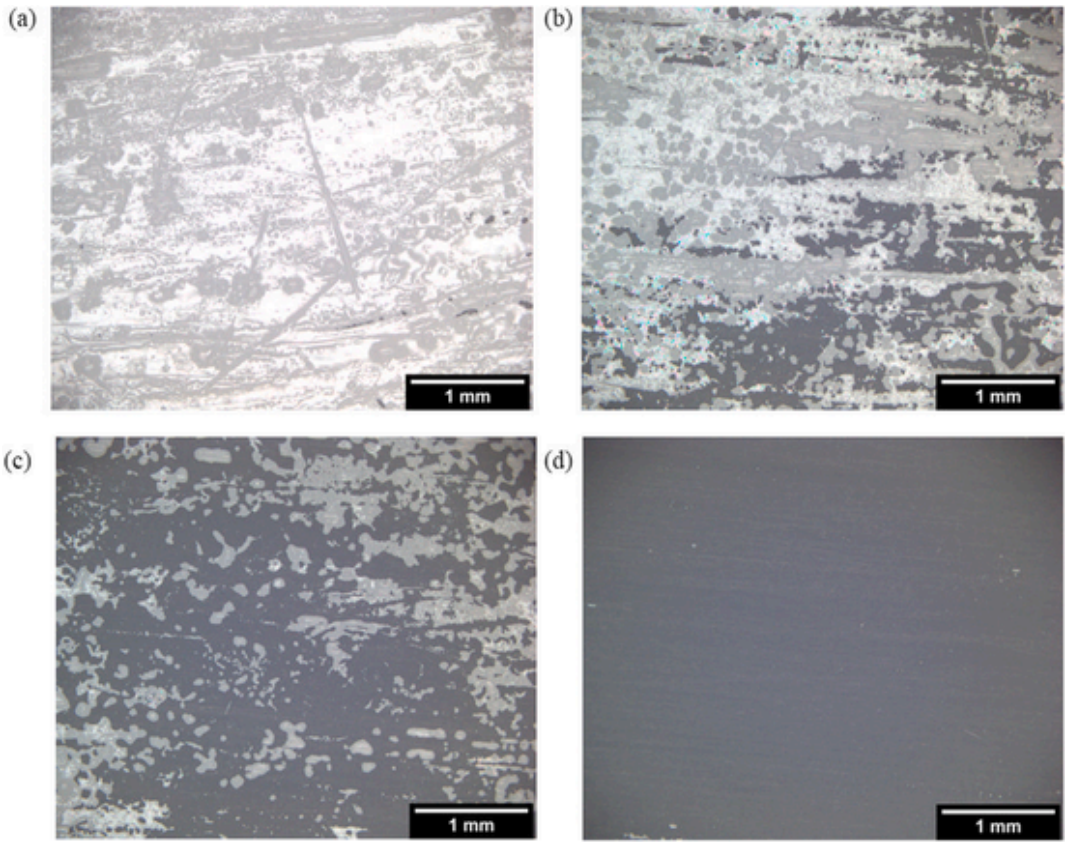

Fig. 6. Representative optical micrographs exhibiting the evolution of contact area between prepreg and glass surface at selected test conditions: (a) 10 °C, 500 mm min^{-1} (DoIC = 0%), (b) 20 °C, 500 mm min^{-1} (DoIC = 26%), (c) 20 °C, 300 mm min^{-1} (DoIC = 75%), and (d) 50 °C, 50 mm min^{-1} (DoIC = 100%). The DoIC value for each micrograph was determined using the circular ROI as illustrated in Fig. 3(b). All micrographs shown here were acquired from the middle glass slide located on the steel substrate (see Fig. 2(a)), at the same location for each glass slide.

surfaces. The strength of developing bonds depends on both the chemical properties and the surface characteristics (e.g. morphology and roughness) which varies between polymer-to-metal and polymer-to-polymer adhesion [13]. For prepreg-prepreg pairing, polymer diffuses between the resin layers of the prepreg surfaces in contact under compaction, effectively forming a single layer that increases adhesion [13]. Moreover, the resin-to-resin contact between two prepreg layers promotes greater contact area. These factors contribute to higher $F_{t,max}$ for prepreg-prepreg pairing when compared to prepreg-steel.

The successful construction of the DoIC master curve shown in Fig. 7 (b) provides confirmation that the DoIC depends on the viscoelastic properties of the resin in the same way as the tack. The experimental set-up leads to a contact time that is approximately inversely proportional to the feed rate, such that high feed rates produce low contact times and vice versa. Whether a resin bonds to a substrate depends on the contact time as well as on the polymer mobility, which is itself temperature dependent. The process of TTS used in creating the master-curve combines these effects into the shifted feed rate. Hence, at higher shifted feed rates (equivalent to lower temperatures), there is insufficient time and mobility for the polymer to relax and to form bonds [2], leading to low DoIC. At lower shifted feed rates (equivalent to increasing temperatures), there is greater contact time and mobility leading to higher DoIC. The scatter reflected in the error bars observed in Fig. 7 is attributed to local variations in the distribution of the resin and in the prepreg thickness (leading to contact pressure variations) [8]. The scatter is also associated with the limited area that can be probed using optical microscopy, despite the number of images recorded per sample. The authors attempted to use a lower magnification surface scanner in order to increase the area imaged, but it was found not possible to produce lighting suitable to identify intimate contact at the prepreg-glass interface.

In an effort to interpret the relationship between tack and DoIC for comparable surface combinations of prepreg and a rigid surface, Fig. 8 plots the tack measurements for prepreg-steel as a function of DoIC obtained from prepreg-glass, at matching test conditions of temperature, feed rates and compaction force. The short timescale between the compaction and acquisition of the micrographs ensures that DoIC is relevant to the test conditions and reduces the effect of surface tension or residual stresses on the contact patterns. The trend observed in Fig. 8 reveals the same transition from adhesive to cohesive failure with decreasing shifted rate as observed in tack master curves (see Fig. 5(a)), but now related to changes in DoIC. The low tack and low DoIC to the left of the peak in Fig. 8 corresponds to the adhesive failure region (high shifted rates in the tack master curves). In this region, tack increases with contact area towards $F_{t,max}$, as expected. Before reaching complete contact, maximum tack corresponds to 74% DoIC. However, on the right side of $F_{t,max}$, the cohesive failure region, further increases in DoIC towards complete contact between the prepreg and glass surface take place simultaneously with a decrease in tack. This is attributed to the increase in molecular mobility of the resin that decreases the resin viscosity. For probe tack tests, Gillanders et al. reported a strong correlation between tack and contact area in PSA tape, determined at a fixed separation rate and temperature [2]. This trend is comparable to the curves in Fig. 8 for the adhesive failure region (left of the peak).

Although images are acquired between 5 and 15 min post compaction, in the absence of large driving forces (such as the compaction pressure) significant changes to the contact area are not expected to arise due to residual stresses and surface tension effects since the viscos-

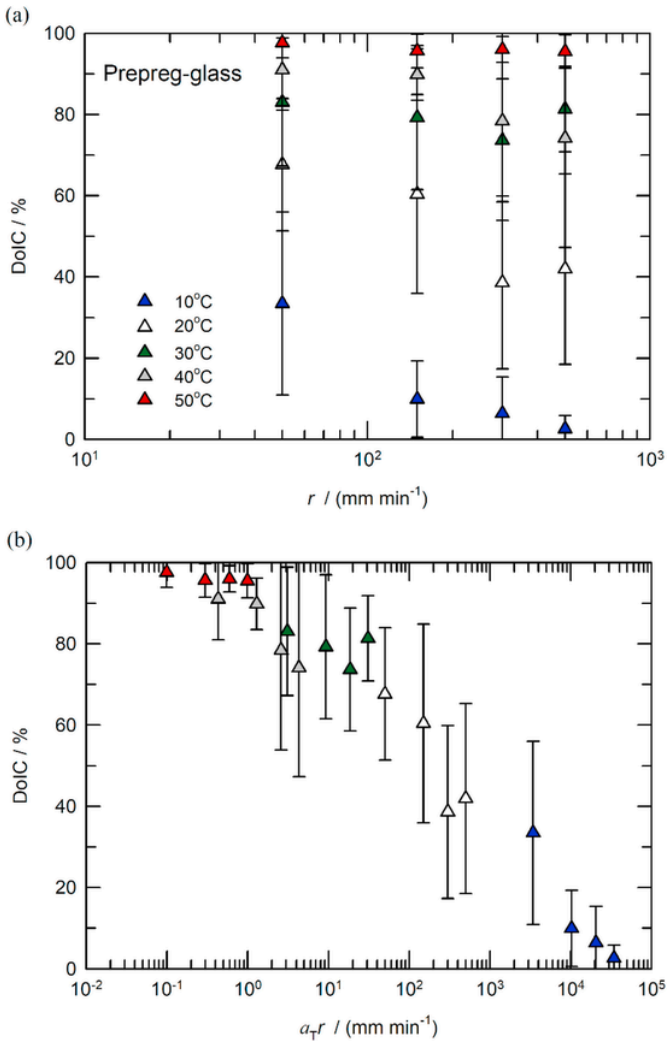

Fig. 7. (a) Degree of intimate contact, DoIC, for prepreg-glass pairing acquired at different temperatures, T, and feed rates, r; average values and standard deviations are indicated. (b) The same DoIC data shifted to T_{ref} = 20 °C using shift factors, a_T, determined from Eq. (1) (see Fig. 4).

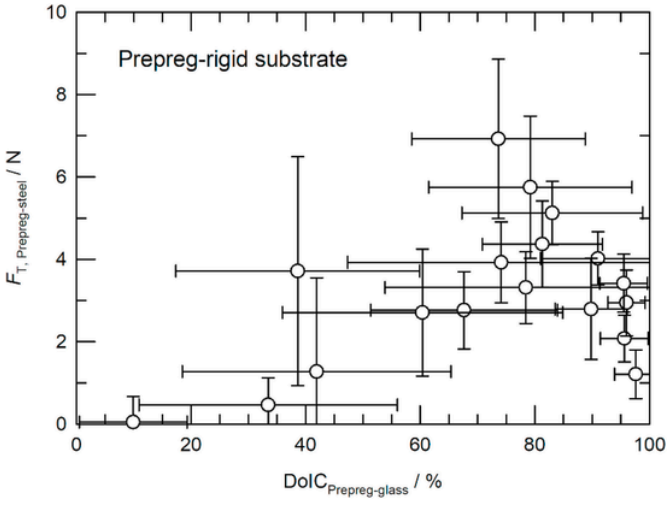

Fig. 8. Tack as a function of DoIC for prepreg-rigid substrate combination acquired using the continuous application-and-peel test, whereby tack was determined from prepreg-steel whereas DoIC was determined from prepreg-glass interface.

ity of the pre-pregged resin is relatively high, but it is acknowledged that small contact area changes may have occurred during this time.

With the present technique it is not possible to obtain a measure of DoIC between two adhering prepreg layers. A combination of ultrasound and X-ray tomography inspection might be able to provide insight into the prepreg-prepreg interface to infer contact area and on the porosity distribution on the surface [14,15] whilst the cross-section tomographs can reveal details of inter-ply porosity [16]. It is, however, reasonable to expect some correlation between prepreg-prepreg tack and DoIC measured on prepreg-glass since they both depend on the same resin viscoelastic properties. This is evidenced by the similarity of the shifted rate at maximum tack between the prepreg-steel and the prepreg-prepreg tack measurements as reported in Table 1. The findings suggest that the molecular mechanism of bond formation for both surface combinations is similar in nature. Therefore, in an effort to estimate the transition from cohesive to adhesive failure for prepreg-prepreg interfaces, it is useful to explore the relationship between prepreg-prepreg tack and DoIC of prepreg-glass.

Fig. 9 shows the prepreg-prepreg tack data plotted against the DoIC of prepreg-glass determined from matching test conditions. It is acknowledged that the substrates for the tack and the DoIC experiments are dissimilar, and hence the difference in surface morphology and surface energies may influence the true contact area, particularly at elevated temperatures. Nevertheless, the comparable trends observed between Figs. 8 and 9 for the different substrate surfaces imply that the influence of temperatures and feed rates on the contact area of prepreg-glass pairing are also relevant to prepreg-prepreg tack.

This study has shown that maximum contact area does not necessarily coincide with maximum tack, due to the balance between the viscoelastic properties of the resin enabling adhesion and cohesive failure. This suggests that efforts to reduce defect formation in AMP should focus on determining the maximum tack for the prepreg material under relevant conditions rather than emphasising maximum DoIC. Despite high DoIC, tack levels in the cohesive failure region vary considerably. This highlights the benefit of employing the tack master curve to supplement the visual examination of the contact area, enabling manufacturers to make informed decisions on AMP prepreg deposition parameters, and to consider other factors that can influence preform manufacture such as material aging and environmental conditions [8,9].

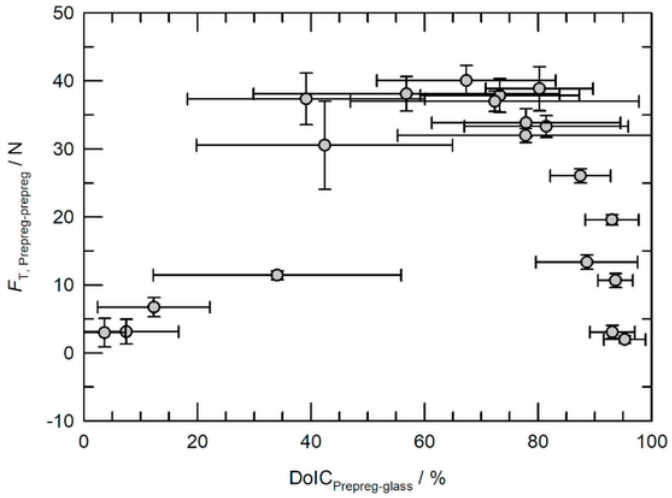

Fig. 9. Tack for prepreg-prepreg combination determined using the continuous application-and-peel test as a function of DoIC determined from prepreg-glass interface.

6. Conclusions

Tack was measured between prepreg and two different substrate surfaces using a continuous test method that couples the application and peel stages at different feed rates and temperatures. Rheometry was performed on the prepreg, to determine the time-temperature dependence of the resin system and modelled using the WLF equation. Tack master curves were constructed by applying TTS to the tack data. Maximum tack and the corresponding feed rate, for both prepreg–steel and prepreg–prepreg pairings, were derived from fitted Gaussian curves and used to quantitatively describe tack behaviour. The maximum tack recorded for prepreg-prepreg is significantly higher than prepreg–steel tack due to the different molecular interactions at prepreg–steel and prepreg–prepreg interfaces. On the other hand, the feed rates at maximum tack for both surface combinations are of a similar order of magnitude.

The contact evolution was studied between prepreg and a glass surface. Application of the prepregs to glass was performed at matching conditions to the prepreg tack measurements, with omission of the peel phase allowing images of the contact area to be acquired. The influence of feed rate and temperature on the prepreg-glass interface was evidenced by quantification of the contact area from optical micrographs using image analysis to yield DoIC. Using the same TTS parameters as applied to the tack data, DoIC master curves were constructed, suggesting that contact formation is also dependent on resin viscoelasticity. The shifted DoIC data revealed that true contact area increased with decreasing shifted feed rates until maximum contact area is reached.

The relationship between DoIC and tack was explored, revealing that both prepreg-steel and prepreg-prepreg pairings manifest similar trends, with tack increasing to a maximum and subsequently decreasing as DoIC increased to maximum contact. In the adhesive failure region, tack increased with DoIC as shifted rates decreased. At lower shifted feed rates, the peel mechanism changed to cohesive failure, and tack reduced regardless of the high level of DoIC due to the enhanced molecular mobility dominating the failure. This shows that maximising DoIC may be an insufficient criterion for optimising AMP processes, and that the prepreg tack master curve is more relevant in informing manufacturing decisions for AMP prepreg deposition.

Acknowledgements

The authors acknowledge the kind contribution of the Hexcel Corporation (Dublin, CA, USA) in providing the materials used in this study. This research did not receive any specific grant from funding agencies in the public, commercial, or not-for-profit sectors.

Appendix A.

An example of a raw force-displacement tack curve illustrating the process of determining the tack force from the measured tensile forces during a tack test is shown in Fig. A1.

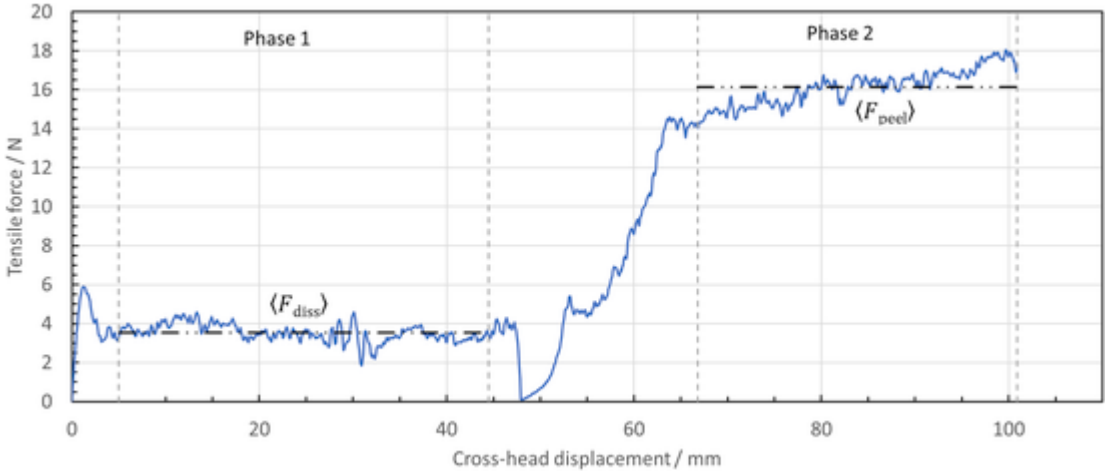

Fig. A1. Measured tensile force as a function of the cross-head displacement during a tack test for a surface combination of prepreg and steel at 40 °C and 50 mm min^{-1}; the specimen width was 75 mm, and the compaction force 100 N. Vertical dashed lines represent the limits for the ranges used to determine the average force values (shown as horizontal dot dot dash lines) for each phase of the tack test.

References

[1] Budelmann D, Schmidt C, Meiners D Prepreg tack: a review of mechanisms, measurement, and manufacturing implication. Polym Compos 2020;41:3440–58. https://doi.org/10.1002/pc.25642.

[2] Gillanders AM, Kerr S, Martin TJ Determination of prepreg tack. Int J Adhesion Adhes 1981;1:125–34. https://doi.org/10.1016/0143-7496(81)90035-X.

[3] Lakrout H, Sergot P, Creton C Direct observation of cavitation and fibrillation in a probe tack experiment on model acrylic pressure-sensitive-adhesives. J Adhes 1999;69:307–59. https://doi.org/10.1080/00218469908017233.

[4] Horgnies M, Darque-Ceretti E, Felder E Relationship between the fracture energy and the mechanical behaviour of pressure-sensitive adhesives. Int J Adhesion Adhes 2007;27:661–8. https://doi.org/10.1016/j.ijadhadh.2006.12.002.

[5] Creton C, Ciccotti M Fracture and adhesion of soft materials: a review. Rep Prog Phys 2016;79:046601. https://doi.org/10.1088/0034-4885/79/4/046601.

[6] Crossley RJ, Schubel PJ, Warrior NA The experimental determination of prepreg tack and dynamic stiffness. Composites Part A 2012;43:423–34. https://doi.org/10.1016/j.compositesa.2011.10.014.

[7] Crossley RJ, Schubel PJ, De Focatiis DSA Time–temperature equivalence in the tack and dynamic stiffness of polymer prepreg and its application to automated composites manufacturing. Composites Part A 2013;52:126–33. https://doi.org/10.1016/j.compositesa.2013.05.002.

[8] Endruweit A, Choong GYH, Ghose S, Johnson BA, Younkin DR, Warrior NA, et al. Characterisation of tack for uni-directional prepreg tape employing a continuous application-and-peel test method. Composites Part A 2018;114:295–306. https://doi.org/10.1016/j.compositesa.2018.08.027.

[9] Smith AW, Endruweit A, Choong GYH, De Focatiis DSA, Hubert P Adaptation of material deposition parameters to account for out-time effects on prepreg tack. Composites Part A 2020;133:105835. https://doi.org/10.1016/j.compositesa.2020.105835.

[10] Helmus R, Kratz J, Potter K, Hubert P, Hinterhölzl R An experimental technique to characterize interply void formation in unidirectional prepregs. J Compos Mater 2016;51:579–91. https://doi.org/10.1177/0021998316650273.

[11] Choong GYH, De Focatiis DSA, Hassell DG Viscoelastic melt rheology and time–temperature superposition of polycarbonate–multi-walled carbon nanotube nanocomposites. Rheol Acta 2013;52:801–14. https://doi.org/10.1007/s00397-013-0706-6.

[12] Williams ML, Landel RF, Ferry JD The temperature dependence of relaxation mechanisms in amorphous polymers and other glass-forming liquids. J Am Chem Soc 1955;77:3701–7. https://doi.org/10.1021/ja01619a008.

[13] Voyutskii SS, Vakula VL The role of diffusion phenomena in polymer-to-polymer adhesion. J Appl Polym Sci 1963;7:475–91. https://doi.org/10.1002/app.1963.070070207.

[14] Fariñas MD, Gómez Álvarez-Arenas TE, Cuevas Aguado E, García Merino M Non-contact ultrasonic inspection of CFRP prepregs for aeronautical applications during lay-up fabrication. 2013 IEEE international ultrasonics symposium (IUS); 2013. p. 1590–3.

[15] Thomas S, Bongiovanni C, Nutt SR In situ estimation of through-thickness resin flow using ultrasound. Compos Sci Technol 2008;68:3093–8. https://doi.org/10.1016/j.compscitech.2008.07.012.

[16] Torres JJ, Simmons M, Sket F, González C An analysis of void formation mechanisms in out-of-autoclave prepregs by means of X-ray computed tomography. Composites Part A 2019;117:230–42. https://doi.org/10.1016/j.compositesa.2018.11.010.